

Agouti-Related Protein Segments Outside of the Receptor Binding Core Are Required for Enhanced Short- and Long-term Feeding Stimulation

Michael E. Madonna,[†] Jennifer Schurdak,[‡] Ying-kui Yang,[§] Stephen Benoit,[‡] and Glenn L. Millhauser^{†,*}

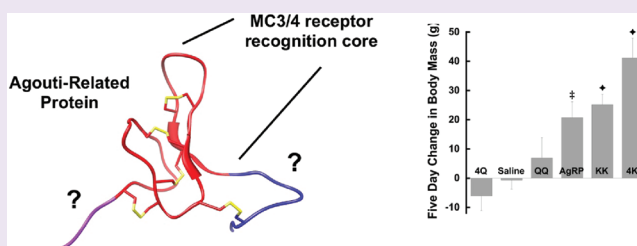
[†]Department of Chemistry and Biochemistry, University of California, Santa Cruz, California 95064, United States

[‡]Department of Psychiatry, University of Cincinnati, Cincinnati, Ohio 45237, United States

[§]Department of Surgery, University of Alabama at Birmingham, Birmingham, Alabama 35205, United States

S Supporting Information

ABSTRACT: The agouti-related protein (AgRP) plays a central role in energy balance by reducing signaling through the hypothalamic melanocortin receptors (McRs) 3 and 4, in turn stimulating feeding and decreasing energy expenditure. Mature AgRP(83–132), produced by endoproteolytic processing, contains a central region that folds as an inhibitor cystine knot (ICK) stabilized by a network of disulfide bonds; this domain alone carries the molecular features for high affinity McR binding and inverse agonism. Outside of the ICK domain are two polypeptide segments, an N-terminal extension and a C-terminal loop, both completely conserved but of unknown function. Here we examine the physiological roles of these non-ICK segments by developing a panel of modified AgRPs that were administered to rats through intracerebroventricular (ICV) injection. Analysis of food consumption demonstrates that basic (positively charged) residues are essential for potent short- and long-term AgRP stimulated feeding. Moreover, we demonstrate an approximate linear relationship between protein charge density and 24 h food intake. Next, we developed artificial AgRP(83–132) analogues with increased positive charge and found that these species were substantially more potent than wild type. A single dose of one protein, designated AgRP-4K, results in enhanced feeding for well over a week and weight gain that is nearly double that of AgRP(83–132). These studies suggest new strategies for the development of potent orexigenic species and may serve as leads for the development of therapeutics for treating wasting conditions such as cachexia.



The agouti-related protein (AgRP) is produced in the hypothalamus and acts to stimulate feeding and decrease energy expenditure.^{1,2} AgRP is a high affinity inverse agonist of the melanocortin 3 and 4 receptors (Mc3R and Mc4R), members of the G-protein coupled receptor (GPCR) superfamily. Transgenic mice that overexpress AgRP exhibit increased feeding, profound weight gain, and metabolic imbalances often associated with diabetes.³ In humans, AgRP plasma levels correlate with body mass,⁴ while certain polymorphisms predispose individuals to anorexia nervosa.^{5,6} Because of its potency in stimulating feeding, leading to weight gain, AgRP and its mimetics are considered prime therapeutic leads in the treatment of cachexia, the wasting condition associated with cancer and AIDS.⁷

There are a number of designed ligands that stimulate feeding, including SHU9119, THP, MBP10, and NBI-30,⁸ but none are more potent after a single low dose administration than AgRP. Moreover, AgRP's effects are prolonged. A single intracerebroventricular (ICV) AgRP injection produces enhanced feeding for up to 7 days,⁹ and animals receiving a dose of AgRP followed 24 h later by administration of MTII (a melanocortin agonist) return to elevated feeding levels at 48 h (24 h after agonist injection).¹⁰

AgRP is produced as a 132 amino acid pro-protein that undergoes proprotein convertase (PC 1/3) cleavage, following residue 82, to release its cysteine-rich C-terminal domain (Table 1).^{11,12} The 10 cysteine residues within AgRP(83–132) form a network of five disulfide bonds, as shown in Figure 1.¹³ Structure determination by NMR demonstrates that residues 87–120 adopt an inhibitor cystine knot (ICK) fold, a scaffold previously found exclusively in invertebrate toxins.¹³ AgRP is homologous to the agouti signaling protein (ASIP), which is expressed in the skin and controls pigmentation by suppressing signaling through Mc1R. Both proteins share the ICK core region in their respective C-terminal domains.¹⁴ In contrast to AgRP, however, the ASIP N-terminal domain is retained and binds to attractin, an interaction that is essential for *in vivo* function.¹⁵

In addition to Mc1R binding, ASIP is also capable of high affinity interactions with Mc3R and Mc4R, as demonstrated by the obese phenotype in the lethal yellow *A^{y/a}* mouse.³ In contrast, AgRP binds exclusively to Mc3R and Mc4R.² We

Received: September 5, 2011

Accepted: November 30, 2011

Published: November 30, 2011



Table 1. Agouti Related Protein Sequences^a

	N-term	Inhibitor Cystine Knot Core	C-Term Loop
Human (83-132)	SSRR	CVRLHESCLGQQVPCCDPCATCYCRFFNAFCYC	RKLGTAMNPCSRT
Cow	SPRR	CVRLHESCLGHQVPCCDPCATCYCRFFNAFCYC	RKLGTNTNPCSRT
Mouse	SPRR	CVRLHESCLGQQVPCCDPCATCYCRFFNAFCYC	RKLGTATNLCSRT
Rat	SPRR	CVRLHESCLGQQVPCCDPCATCYCRFFNTFCYC	RKLGTGTNLCSRP
Pig	SPRR	CVRLHESCLGHQVPCCDPCATCYCRFFNAFCYC	RKLGTATNPCSRT
Sheep	SPRR	CVRLHESCLGHQVPCCDPCATCYCRFFNAFCYC	RKLGTNT

Designed AgRP Sequences

AgRP(83-120)	SSRR	CVRLHESCLGQQVPCCDPAATCYCRFFNAFCYC	R
AgRP(87-132)		CVRLHESCLGQQVPCCDPCATCYCRFFNAFCYC	RKLGTAMNPCSRT
AgRP(87-120)		CVRLHESCLGQQVPCCDPAATCYCRFFNAFCYC	R
AgRP-2Q	SSRR	CVRLHESCLGQQVPCCDPCATCYCRFFNAFCYC	RQLGTAMNPCSQT
AgRP-4Q	SSQQ	CVRLHESCLGQQVPCCDPCATCYCRFFNAFCYC	RQLGTAMNPCSQT
AgRP-2K	SSRR	CVRLHESCLGQQVPCCDPCATCYCRFFNAFCYC	RKLKTKMNPCSRT
AgRP-4K	KKRR	CVRLHESCLGQQVPCCDPCATCYCRFFNAFCYC	RKLKTKMNPCSRT

Basic residues in the N-terminal segment and C-terminal loop are shown in blue.

^aBasic residues in the N-terminal segment and C-terminal loop are shown in blue.

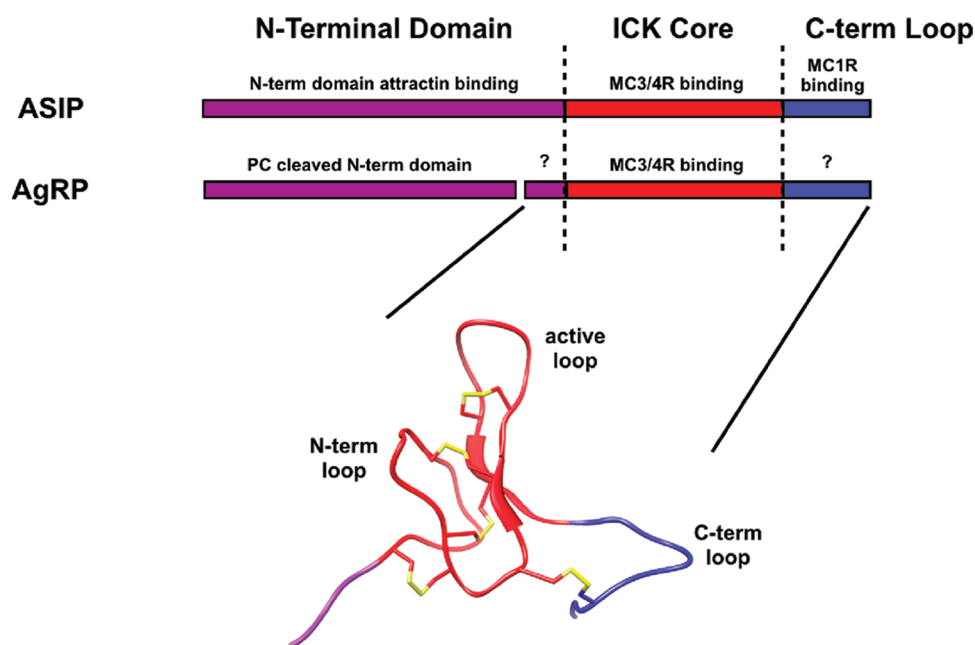


Figure 1. Schematic of ASIP and AgRP structure/function. The sequence diagram (above) illustrates homologous regions of the two proteins and corresponding functional domains. Question marks indicate the two regions of AgRP of conserved but otherwise unknown function. Structure of AgRP(83-132) (below) illustrates the spatial location of the different regions.

recently reported a study using a panel of ASIP/AgRP chimeras with the goal of identifying the specific features in ASIP required for Mc1R affinity.¹⁶ We found that the ASIP C-terminal loop, just past the ICK core, was critical for Mc1R recognition. Moreover, grafting this loop onto the AgRP ICK core resulted in a protein with a Mc1R K_d of approximately 30 nM. As shown in Figure 1, these studies now complete the characterization of ASIP's functional domains.

In contrast, the functions of the polypeptide segments outside of AgRP's ICK core are unknown (Figure 1). The four residue segment preceding the ICK core (Ser-Ser-Arg-Arg) and the 13 residue C-terminal loop are both highly conserved

among mammals (Table 1), yet deletion of these segments has absolutely no effect on the Mc3R or Mc4R binding affinities or in vitro activity.¹⁷ Specifically, a mini protein composed of just the AgRP ICK core, residues 87-120, possesses approximately the same Mc3R and Mc4R affinity as AgRP(87-132)¹⁷ and AgRP(83-132)¹⁸ and exhibits equivalent inverse agonism.¹⁹ AgRP is a strongly cationic protein, and interestingly, five of the seven positively charged amino acids are located in the regions outside of the ICK core (defined by the first and last Cys residues).

To address the functional significance of the segments outside of the ICK core domain in mature AgRP(83-132)

(Figure 1), we performed ICV experiments on Long-Evans rats using a panel of AgRP variants in which select non-ICK components are deleted. We find a remarkable relationship between long-term feeding enhancement and net AgRP positive charge, carried mainly by the non-ICK segments. Next, we developed a series of novel AgRP constructs where charge is selectively varied. ICV experiments with these constructs not only support the charge-feeding relationship but also lead to the discovery of an AgRP analogue that significantly increases initial and long-term feeding relative to the wild type protein. Together, these studies demonstrate a critical physiological role for the non-ICK AgRP segments and suggest new strategies in the development of reagents for treating cachexia and other conditions associated with negative energy balance.

■ RESULTS AND DISCUSSION

Truncated AgRP Variants. ICV injection of AgRP variants was used to assess the physiological role of the protein segments outside of the ICK core, comprising the receptor binding domain (Figure 1). Initial experiments focused on truncated forms of mature AgRP(83-132) (Table 1). The minimal construct AgRP(87-120) was designed and investigated in a previous study.¹⁷ Briefly, this protein lacks both the four residue segment before the ICK domain, and the C-terminal loop. Simple elimination of the C-terminal loop leaves an uncompensated Cys residue at position 105. To avoid the formation of non-native disulfide bonds, residue 105 was mutated to Ala. In addition, Arg120 following the penultimate Cys was retained as it is part of the β -sheet. Our previous NMR work showed that AgRP(87-120), often referred to as mini-AgRP, folds 100% to a uniform product that retains the ICK structure of the parent protein.¹⁷ Moreover, dissociation constants measured at Mc3R and Mc4R are equivalent to mature AgRP(83-132). Two other constructs, AgRP(83-120) and AgRP(87-132) were prepared using the same strategies.

ICV injections were administered to Long-Evans rats fitted with cannulas in the third ventricle. Proteins were delivered as a single 1.0 nmol dose in 1.0 μ L of solution. Feeding and weight were monitored in most cases until consumption returned to baseline values. Results for wild type AgRP(83-132) and the three truncated variants are shown in Figure 2A. All initially stimulate feeding, as seen in the responses after 1 day. AgRP(83-132) is the most potent, stimulating feeding nearly 80% over that of control ($P < 0.001$), while mini-AgRP is the least potent. Interestingly, AgRP(83-120) is essentially equipotent to wild type ($P < 0.001$). At 3 or 4 days after injection, enhanced feeding relative to control diminishes. Animals dosed with the three truncated variants are almost back to baseline. In contrast, those treated with AgRP(83-132) are still consuming feed about 30% over control ($P < 0.05$ at day 4).

The data in Figure 2A suggest that the four residue non-ICK segment preceding the ICK core is required for rapidly stimulating feeding, whereas both non-ICK segments are needed for long-term effects. The significant number of basic, positively charged residues carried in the non-ICK segments motivated us to examine the relationship between 24 h feeding and charge per residue (total protein charge divided by the number of amino acids) for the four proteins, as shown in Figure 2B. Interestingly, there is an approximate linear relationship, with a near 4-fold increase in feeding from a doubling of the protein charge density.

Charge-Modified AgRP Variants. We further tested the role of charge with a series of mutations in full AgRP(83-132). To eliminate positive charges, we replaced Arg or Lys with Gln, which retains local side chain steric features and preserves solubility in aqueous solution (Table 1). AgRP-2Q lacks two charges in the C-terminal loop, whereas AgRP-4Q lacks charges in both the N-terminal segment and the C-terminal loop. Feeding behavior after ICV injection is shown in Figure 3A. Both AgRP and AgRP-2Q greatly stimulate feeding in the first 24 h. Consistent with the data of Figure 2, basic residues within the C-terminal loop are not important for the initial feeding response. Interestingly, AgRP-2Q is somewhat more potent than wild type in both short- and long-term feeding responses. In contrast, AgRP-4Q gives a weak 24 h response ($P < 0.05$) and returns to baseline after the second day. AgRP-4Q elicits responses similar to that of AgRP(87-120) demonstrating that elimination of the non-ICK segments, or simply the basic residues within these segments, is sufficient to reduce both short- and long-term potency.

To further test the relationship between positive charge and feeding stimulation, we developed AgRP analogues with additional Lys residues. Inspection of the wild type AgRP(83-132) three-dimensional structure reveals a cluster of basic residues extending from the active loop (Figure 1) to the end of the C-terminal loop, as shown in Figure 4. We reasoned that this conserved spatial arrangement could play a part in the feeding enhancement observed for AgRP(83-132) relative to AgRP(83-120). Consequently, we considered positions contiguous with this cluster. Among the possible positions, we chose to mutate Gly123 and Ala125 since these amino acids lack side chain functional groups and are therefore unlikely to play a structural role. The resulting double mutant is referred to as AgRP-2K. We additionally replaced the two Ser residues in the N-terminal segment with Lys, giving the AgRP-4K analogue.

The results following ICV injection of AgRP-2K and AgRP-4K are striking, as shown in Figure 3B. AgRP-2K elicits an approximate 50% increase in food uptake relative to wild type AgRP in the first 24 h ($P < 0.001$) and continues to stimulate feeding out to 6 or 7 days. The initial response from AgRP-4K is similar to that of AgRP-2K, but here the animals display elevated feeding beyond 9 days, at which point the experiments were halted ($P < 0.05$ at day 8). The relationship between 24 h feeding and charge density in the Gln and Lys mutants is displayed in Figure 3C and supports linear behavior observed for the truncated AgRP variants. Finally, we examined the change in body mass 5 days after injection, as shown in Figure 4D. The results parallel the relationship observed between charge and 24 h feeding (Figure 3E), with AgRP-4Q giving a slight decrease in body mass, and AgRP-4K giving by far the greatest increase. Moreover, AgRP-4K leads to an increase in body mass that is approximately double that observed for wild type AgRP(83-132). ICV data are fully summarized in Table 2.

Mc3R and Mc4R Pharmacology. We used both displacement and activity assays to evaluate the influence of truncation or charge alteration on receptor pharmacology. Measurements were performed on HEK293 cells expressing the desired receptor subtype. Figure 5 shows ¹²⁵I-NDP-MSH displacement for all variants at Mc3R and Mc4R, with K_i values and errors reported in Table 3. Variation is limited from 4.5 to 16 nM at Mc3R and from 7.6 to 16 nM at Mc4R. The variants that give the strongest feeding response fall in the middle of the K_i range and, in general, do not suggest any relationship between

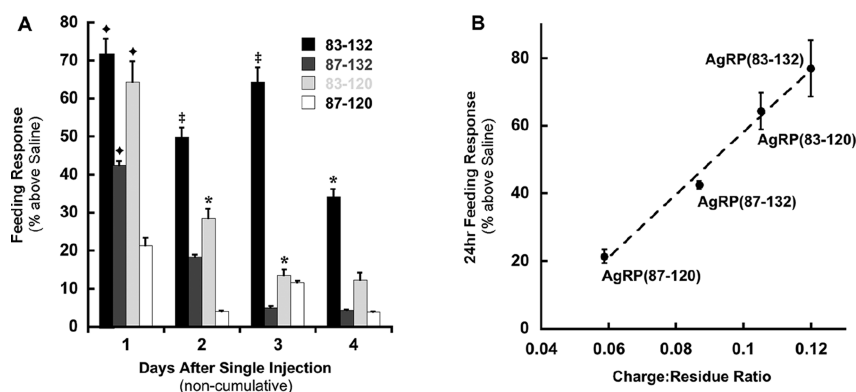


Figure 2. Effect of a single administration of a 1.0 mmol dose of wild type and truncated AgRPs into the third cerebral ventricle in male Long-Evans rats. (A) Percent increase over saline at 24, 48, 72, and 96 h after injection (noncumulative). (B) Net charge density trend of 24 h feeding response above saline control. ♦ $P < 0.001$, † $P < 0.01$, and * $P < 0.05$.

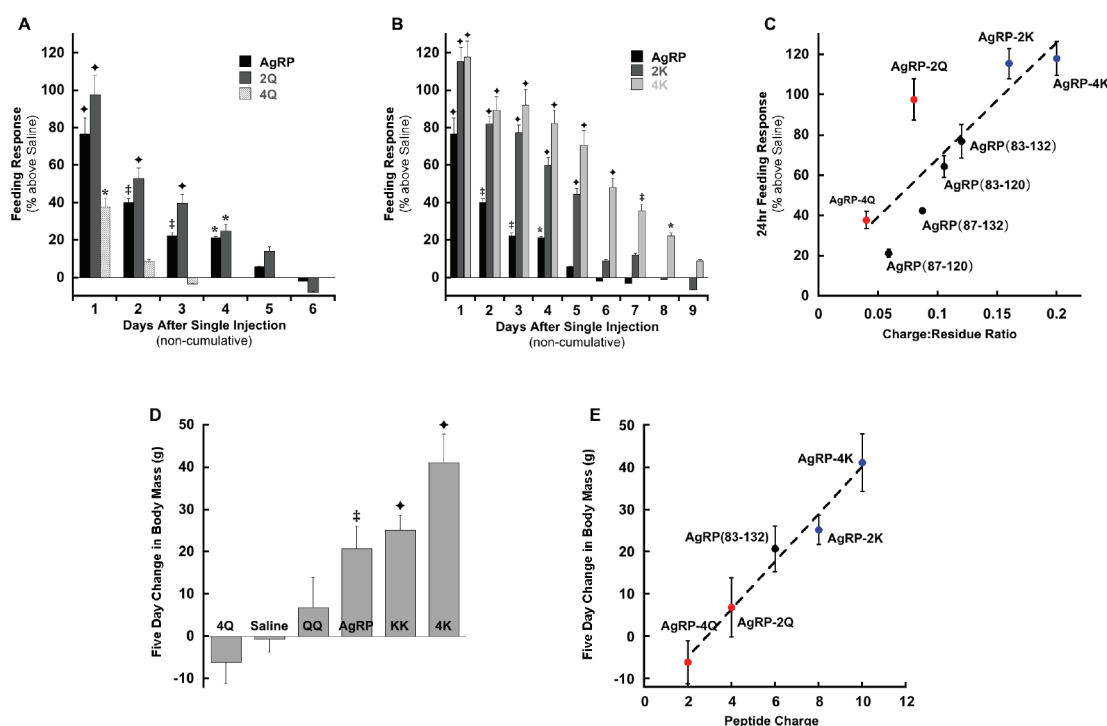


Figure 3. Effect of a single administration of a 1.0 mmol dose of mutated and designed AgRPs into the third cerebral ventricle in male Long-Evans rats. (A and B) Noncumulative percent increase of feeding response compared to saline of AgRP proteins with modified charges. (C) Relationship between 24 h feeding and net charge density for all AgRP constructs. (D) 5-Day change in body mass and (E) trend in net peptide charge and 5-day change in body mass. ♦ $P < 0.001$, † $P < 0.01$, and * $P < 0.05$ vs saline.

dissociation constant and short-term or long-term consumption. Each variant was further evaluated for its ability to suppress NDP-MSH stimulated cAMP production. Antagonists give a rightward shift in the response curve. The resulting curves are shown in Figure 5, with EC_{50} values and errors in Table 3. The EC_{50} values also exhibit limited variation, although greater than observed for the displacement studies, and range from 1.6 to 16 nM at Mc3R and 1.7 to 17 nM at Mc4R. Interestingly, the lowest EC_{50} values at both receptors are observed for the AgRP-4Q and AgRP-4K variants, which elicit opposite feeding responses. In general, these results are consistent with our previous work, which found equivalent receptor affinity between AgRP(87-120) and AgRP(87-132), and demonstrate that receptor affinity or activity cannot

account for the broad range of *in vivo* responses observed for the panel of AgRP variants.

Possible Mechanisms and Implications. The findings above identify an unanticipated but nevertheless dramatic functional role for the AgRP polypeptide segments outside of the ICK core domain. Comparison of wild type AgRP to a mini-AgRP, composed of only the ICK core, shows that the Ser-Ser-Arg-Arg N-terminal extension and the C-terminal loop greatly enhance both the initial and long-term feeding responses. Of these two non-ICK segments, the N-terminal extension is more important, especially for the initial feeding response, but both play a role in sustaining feeding levels above baseline. By evaluation of designed AgRP mutants, we further showed that positive charge conferred by basic residues in these segments is responsible for the observed *in vivo* responses.

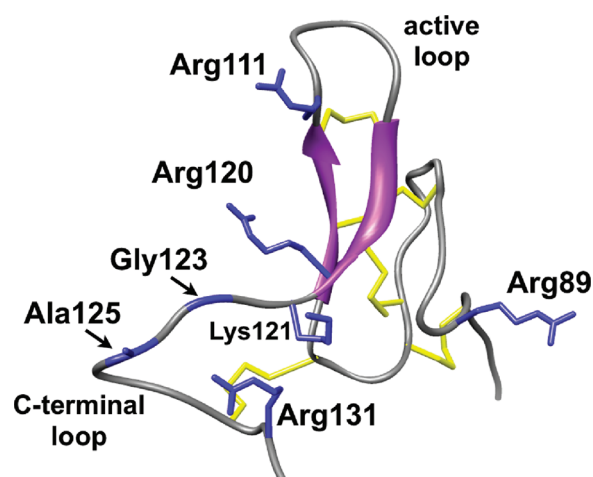


Figure 4. Cluster of basic residues (blue) in AgRP(83-132) from the active and C-terminal loops. AgRP-2K was developed by mutation of Gly123 and Ala125 (arrows) to Arg. Basic residue side chains in the N-terminal segment (Ser⁸³-Ser⁸⁴-Arg⁸⁵-Arg⁸⁶) are not shown.

Inclusion of additional charges beyond those found in wild type results in a protein that generates a profound feeding response that lasts almost twice as long as that induced by the wild type AgRP. It is unlikely that these results arise from modulation in receptor binding affinity, as the measured dissociation constants and cAMP activities at Mc3R and Mc4R exhibit little variation and no correlation with feeding behavior.

Examination of mammalian AgRP sequences reveals some variation in the two non-ICK segments, but always at positions that do not carry positive charge (Table 1).^{12,13} The basic Lys and Arg residues are completely conserved, and acidic residues are never found at sites that do exhibit variation. It is unlikely that these segments play a structural role. Structure determination by NMR, performed by our lab, found that the C-terminal loop is flexible and points away from the ICK core containing four of the five disulfide bonds.¹³ Moreover, the mini-AgRP construct folds cooperatively with stability that is indistinguishable from AgRP(83-132).¹⁷ Interestingly, the mini-AgRP core domain is so stable that it is now being used as a scaffold in protein design.^{20–22}

There is also no evidence that these segments are required for *in vivo* processing to produce mature AgRP(83-132). As noted in the earlier, AgRP is produced as a pro-protein that undergoes processing by the serine endoprotease PC 1/3.^{11,12} AgRP residues 79–82 (Arg-Glu-Pro-Arg) follow the P4-P1 consensus sequence targeting cleavage to the Arg82-Ser83 peptide bond.^{23,24} Alternate cleavage sights are not observed; the processed form of the protein is found exclusively as

AgRP(83-132).²⁵ Moreover, PC 1/3 is tolerant of sequence variations at the P1'-P4' sites (Ser-Ser-Arg-Arg in AgRP) following the cleavage point, thus suggesting a distinct role for the conserved Arg85-Arg86 residues.²³

Among the known collection of natural and synthetic orexigenic peptides, AgRP exhibits the greatest overall potency. For example, a single 1.0 nM dose of neuropeptide Y (NPY) rapidly stimulates feeding beyond that of an equivalent dose of AgRP, but its effects quickly dissipate and feeding returns to baseline after 24 h.^{10,26} The synthetic cyclic hexapeptide SHU9119 gives a long-term response similar to AgRP but requires higher minimal doses for activation.⁸ Because of its unique behavior, AgRP is considered to be an important lead in the development of drugs for treating cachexia.²⁷ Cachexia is a state of negative energy balance that often arises with cancer, AIDS, and kidney failure and leads to malnutrition and loss of body mass.^{7,28} Maintaining positive energy balance, on the other hand, correlates strongly with the outcome of cancer patients undergoing radiation or chemotherapy. Consistent with the role of the melanocortin system in maintaining energy balance, animal models driven to cachexia by tumors or administration of lipopolysaccharide (LPS) resume normal feeding and body weight from the administration of Mc4R antagonists, including AgRP.²⁷ It is therefore noteworthy that our findings here identify new features that enhance AgRP function and prolong efficacy by nearly a factor of 2.

It is clear from our experiments that AgRP's basic residues, outside of the ICK core McR recognition domain, play a central role in modulating short- and long-term AgRP function. Although the direct mechanism linking positive charge to AgRP function is not clear, we note three possibilities: First, the basic residues may increase AgRP diffusibility, thereby moving the protein more efficiently from the ventricle to the hypothalamus. Second, they may slow degradation or facilitate interactions with accessory molecules proximal to the melanocortin receptors. For example, negatively charged syndecans, cell surface proteoglycans, are implicated in McR regulation.^{29,30} New experiments show that AgRP localization in the paraventricular nucleus is reduced in syndecan knockout mice, suggesting that syndecans are required for concentrating AgRP at postsynaptic membranes.³¹ Finally, the basic residues may facilitate signaling through a non-McR pathway. In support of this mechanism, injection of the synthetic agonist MTII, following AgRP administration, transiently reduces feeding, which then returns to the level consistent with AgRP dose.¹⁰ Moreover, loss of feeding regulation, resulting from selective ablation of AgRP neurons, is not reversed by increased ASIP levels.³²

Table 2. ICV Feeding and Body Mass

peptide	24 h feeding (% above saline)	day-3 feeding (% above saline)	day-5 feeding (% above saline)	5-day Δ in body mass (g)
AgRP(83-132)	76.94 \pm 8.4 \blacklozenge	22.24 \pm 0.9 [‡]	5.78 \pm 0.3*	20.7 \pm 5.4 [‡]
AgRP(87-132)	42.4 \pm 1.1 \blacklozenge	5.02 \pm 0.4*		ND ^a
AgRP(83-120)	64.33 \pm 5.4 \blacklozenge	13.49 \pm 1.5*		ND ^a
AgRP(87-120)	21.32 \pm 2 [#]	11.60 \pm 0.5 [#]		ND ^a
AgRP-2Q	97.7 \pm 10.1 \blacklozenge	39.84 \pm 4.6 \blacklozenge	14.07 \pm 2.3 [#]	6.89 \pm 7 [#]
AgRP-4Q	37.9 \pm 4.4*	−3.45 \pm 0.2 [#]		−6.09 \pm 5 [#]
AgRP-2K	115.5 \pm 7.5 \blacklozenge	77.28 \pm 4.3 \blacklozenge	44.51 \pm 3.1 \blacklozenge	25.16 \pm 3.5 \blacklozenge
AgRP-4K	118 \pm 8.3 \blacklozenge	92.27 \pm 8.3 \blacklozenge	70.78 \pm 7.6 \blacklozenge	41.11 \pm 6.8 \blacklozenge

^aNot determined. \blacklozenge $P < 0.001$ vs saline. [‡] $P < 0.01$ vs saline. * $P < 0.05$ vs saline. [#] $P \geq 0.2$ vs saline.

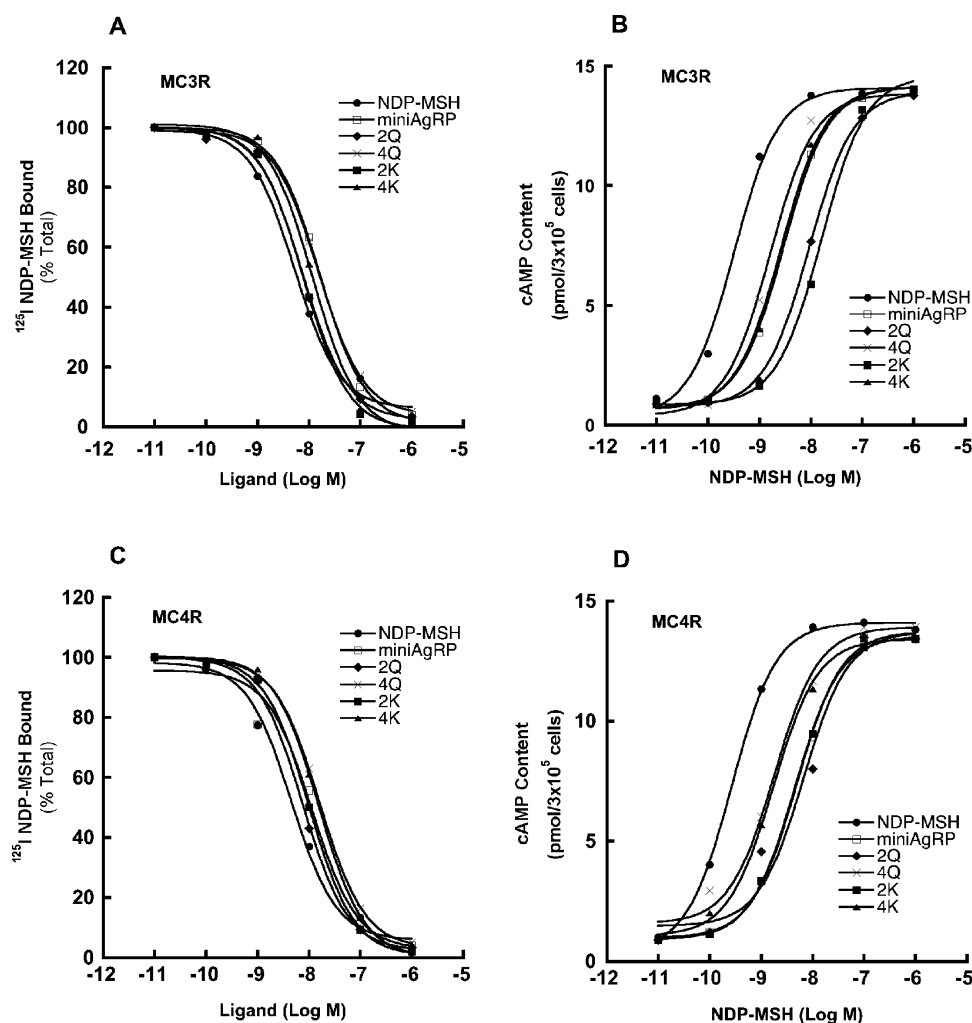


Figure 5. Pharmacology of novel AgRP constructs at Mc3r and Mc4r. (A and C) Displacement of ^{125}I -NDP-MSH; (C and D) cAMP production from increasing NDP-MSH concentrations in the presence of 0.10 μM AgRP proteins.

In summary, we have demonstrated a clear functional role for AgRP's conserved non-ICK segments. The basic, positively charged residues are vital for AgRP stimulated long-term feeding. Enhancement of positive charge in these non-ICK segments leads to a protein of unprecedented orexigenic potency. Moreover, AgRP may be engineered to have variable long-term feeding profiles. Given that the arcuate nucleus is not fully protected by the blood–brain barrier, the potent AgRP-4K protein developed here, or its derivatives, may be deliverable by intravenous injection. In general, the principles identified here will be helpful in pharmaceutical design for treating cachexia and perhaps other conditions associated with improper energy balance.

METHODS

Peptide Synthesis, Purification, and Folding. All peptides were synthesized using Fmoc synthesis on an Applied Biosystems (Foster City, CA) 433A Peptide Synthesizer on a 0.25 mmol scale. Syntheses were monitored using the SynthAssist version 2.0 software package. All peptides were assembled on a Rink-amide-MBHA. Amino acids and resins were purchased through NovaBiochem. HBTU was obtained from Advanced Chemtech (Louisville, KY), and all other reagents were purchased from Sigma-Aldrich (St. Louis, MO). Fmoc deprotection was achieved using a 1% hexamethyleneimine (HMI) and 1% 1,8-diazabicyclo[4.5.0]undec-7-ene (DBU) solution in DMF. Deprotection was monitored by conductivity and continued until the

conductivity level returned to the baseline, then synthesis continued. Deprotection times ranged from 2.5 to 7 min. Couplings used 4 equiv of Fmoc-amino acid in HBTU/DIEA for all amino acids except preactivated Fmoc-Cys(trt)-OPfp. A 3-fold excess of Fmoc-Cys(trt)-OPfp was dissolved in 1.5 mL of 0.5 M HOAt/DMF with no DIEA for coupling. AgRP(87-132) and AgRP(87-120) were N-terminal acetylated by reacting with 0.5 M acetic anhydride in DMF for 5 min. Fully synthesized peptide resins were split into 3 reaction vessels, washed with DCM, and dried. A solution of 12 mL of TFA containing 200 mL each of TIS/EDT/liquesfied phenol (as scavengers) was added to each reaction vessel of dry peptide resin and incubated for 1.5 h. The resin was filtered and washed with 1 mL TFA, and the combined filtrate and wash was then added to 90 mL of cold dry diethyl ether for precipitation. The precipitate was collected by centrifugation, and the ether was discarded. The pellet was dissolved in 40 mL 1:1 $\text{H}_2\text{O}/\text{ACN}$ (0.1% TFA) and lyophilized.

Peptides were purified by RP-HPLC on Vydac (Hesperia, CA) preparative C18 columns. Fractions were collected and analyzed by ESI-MS on a Micromass (Wythenshawe, UK) ZMD mass spectrometer to confirm the correct molecular weight. In each case the major peak was found to be the peptide, and fractions that contained the peptide as a major constituent were combined and lyophilized.

Air oxidative folding of each peptide was accomplished by dissolving the unfolded peptide into folding buffer (2.0 M GuHCl/0.1 M Tris, 3 mM GSH, 400 μM GSSG, pH 8) at a peptide concentration of 0.1 mg/mL and stirring for 24–36 h. Folding was monitored for all

Table 3. Ligand Displacement and EC50 Values

peptide	Mc3R		Mc4R	
	K _i (nM)	EC ₅₀ (nM)	K _i (nM)	EC ₅₀ (nM)
AgRP(87-132)	5.2 ± 0.7 ^b	8.9 ± 0.2 ^d	11 ± 1 ^b	17 ± 3 ^c
AgRP(83-132)	ND ^a	ND ^a	11 ± 0.7 ^c	ND ^a
AgRP(83-120)	16.5 ± 0.4	2.96 ± 0.4	11.4 ± 4	4.92 ± 1.3
AgRP(87-120)	7.5 ± 0.5 ^b	5.5 ± 0.2	6.1 ± 0.5 ^b	13 ± 3 ^c
AgRP-2Q	7.56 ± 1.3	9.22 ± 1.4	7.56 ± 0.3	6.66 ± 2.1
AgRP-4Q	15.6 ± 0.3	1.62 ± 0.3	16.2 ± 0.7	1.8 ± 0.5
AgRP-2K	7.84 ± 0.5	16.1 ± 1.6	9.99 ± 3.7	4.54 ± 1.3
AgRP-4K	11.91 ± 4	2.66 ± 0.3	15.65 ± 1.4	1.72 ± 0.4

^aNot determined. ^bData adapted from Jackson *et al.*¹⁷ ^cData adapted from Patel *et al.*¹⁶ ^dData adapted from Wilczynski *et al.*³⁴ ^eData adapted from Creemers *et al.*¹¹

peptides by RP-HPLC on a C18 analytical column, which revealed a single peak, in each case, for the folded material that was shifted to an earlier retention time than the fully reduced peptide. The folded product was purified by RP-HPLC on a C18 preparative column, and its identity was confirmed as the fully oxidized product by ESI-MS. Reinjecting a small sample of the purified peptide on an analytical RP-HPLC column assessed purity of the peptides. Sample purity was determined to be >90%. Quantitative analysis of the peptide concentrations was done by UV absorption.

Rodent Studies. Male Long-Evans rats ~10–12 weeks old and weighing 250–350 g were obtained from Harlan (Indianapolis, IN) and maintained in an AALAC accredited vivarium on a 12 to 12 h light dark cycle. Animals were given ad libitum access to standard rodent chow and water. After a 1 week habituation period, all animals were deeply anesthetized with a 1 mL/kg dose of (0.22 g Ketamine/0.03 g Xylazine) and placed into a stereotaxic apparatus with the incisor bars set at +1.0. Subsequently, an indwelling cannula was lowered into the third ventricle using the following coordinates, AP = −2.2, ML = 0, DV = −7.0. All animals were allowed to recover for 2 weeks during which time they regained their presurgical body weight. To verify cannula placement, angiotensin II (10 ng/μL) was injected into the third ventricle and water consumption was measured over a 1 h period. To be included animals had to drink more than 7 mL. Animals were injected 1 h prior to the beginning of their dark phase using a within subjects paradigm.

Trials were conducted with one control group (receiving saline) and one experimental group (receiving the peptide of interest). After feeding returned to baseline, animals were allowed to re-equilibrate for 1 week before switching the experimental and control groups and repeating the experiments. Each individual group maintained $n > 5$. The results of all trials were combined to assess percent baseline, due to differences in time of year and animal subjects. Changes in absolute grams of food intake are not different than changes in percent baseline. All experiments were run in replicates of 2–3 studies. Errors are expressed as ± SEM.

Pharmacology. The HEK-293 cell line was used for hMc3R and hMc4R transfection. The cells transfected with receptor were cultured in DMEM medium containing 10% bovine fetal serum and HEPES. Cells at 80% confluence were washed twice, and the receptor constructs were transfected into cells using lipofectamine (Life Technologies, Rockville MD). All experiments were run in triplicate, and errors are expressed as ± SEM (Table 3).

Binding Assays. Binding experiments were performed using the conditions previously described. Briefly, after removal of the media, cells were incubated with nonradioligand NDP-MSH or AGRP analogues from 10^{-10} to 10^{-6} M in 0.5 mL of MEM containing 0.2% BSA and 1×10^5 cpm of 125 I-NDP-MSH for 1 h. The binding reactions were terminated by removing the media and washing the cells twice with MEM containing 0.2% BSA. The cells were then lysed with 0.2 N NaOH, and the radioactivity in the lysate was quantified in an analytical gamma counter (PerkinElmer, Shelton, CT). Nonspecific binding was determined by measuring the amount of 125 I-label bound on the cells in the presence of excess 10^{-6} M unlabeled ligand. Specific

binding was calculated by subtracting nonspecifically bound radioactivity from total bound radioactivity.

cAMP Assays. Cellular cAMP generation was measured using a competitive binding assay kit (TRK 432, Amersham, Arlington Heights, IL). Briefly, cell culture media was removed, and cells were incubated with 0.5 mL of Earle's Balanced Salt Solution (EBSS), containing the melanocortin agonist NDP-MSH (10^{-10} – 10^{-6} M), for 1 h at 37 °C in the presence of 10^{-3} M isobutylmethylxanthine. The reaction was stopped by adding ice-cold 100% ethanol (500 μL/well). cAMP content was measured as previously described, according to instructions accompanying the assay kit.³³

■ ASSOCIATED CONTENT

● Supporting Information

This material is available free of charge *via* the Internet at <http://pubs.acs.org>.

■ AUTHOR INFORMATION

Corresponding Author

*E-mail: glennm@ucsc.edu.

■ ACKNOWLEDGMENTS

The authors thank G. Barsh of Stanford University and the HudsonAlpha Institute for helpful discussion and comments on the manuscript. This work was supported by a grant from the National Institutes of Health (DK064265).

■ REFERENCES

- (1) Kaelin, C. B., Candille, S. I., Yu, B., Jackson, P., Thompson, D. A., Nix, M. A., Binkley, J., Millhauser, G. L., and Barsh, G. S. (2008) New ligands for melanocortin receptors. *Int. J. Obes.* 32 (Suppl 7), S19–27.
- (2) Ollmann, M. M., Wilson, B. D., Yang, Y. K., Kerns, J. A., Chen, Y., Gantz, I., and Barsh, G. S. (1997) Antagonism of central melanocortin receptors in vitro and in vivo by agouti-related protein. *Science* 278, 135–138.
- (3) Wilson, B. D., Ollmann, M. M., and Barsh, G. S. (1999) The role of agouti-related protein in regulating body weight. *Mol. Med. Today* 5, 250–256.
- (4) Katsuki, A., Sumida, Y., Gabazza, E. C., Murashima, S., Tanaka, T., Furuta, M., Araki-Sasaki, R., Hori, Y., Nakatani, K., Yano, Y., and Adachi, Y. (2001) Plasma levels of agouti-related protein are increased in obese men. *J. Clin. Endocrinol. Metab.* 86, 1921–1924.
- (5) Adan, R. A., Hillebrand, J. J., De, R. C., Nijenhuis, W., Vink, T., Garner, K. M., and Kas, M. J. (2003) Melanocortin system and eating disorders. *Ann. N.Y. Acad. Sci.* 994, 267–274.
- (6) Vink, T., Hinney, A., van, E. A. A., van, G. S. H., Sandkuijl, L. A., Sinke, R. J., Herpertz-Dahlmann, B. M., Hebebrand, J., Remschmidt, H., van, E. H., and Adan, R. A. (2001) Association between an agouti-related protein gene polymorphism and anorexia nervosa. *Mol. Psychiatry* 6, 325–328.

- (7) Krasnow, S. M., and Marks, D. L. (2010) Neuropeptides in the pathophysiology and treatment of cachexia. *Curr. Opin. Support. Palliat. Care* 4, 266–271.
- (8) Joppa, M. A., Ling, N., Chen, C., Gogas, K. R., Foster, A. C., and Markison, S. (2005) Central administration of peptide and small molecule MC4 receptor antagonists induce hyperphagia in mice and attenuate cytokine-induced anorexia. *Peptides* 26, 2294–2301.
- (9) Hagan, M. M., Benoit, S. C., Rushing, P. A., Pritchard, L. M., Woods, S. C., and Seeley, R. J. (2001) Immediate and prolonged patterns of Agouti-related peptide-(83–132)-induced c-Fos activation in hypothalamic and extrahypothalamic sites. *Endocrinology* 142, 1050–1056.
- (10) Hagan, M. M., Rushing, P. A., Pritchard, L. M., Schwartz, M. W., Strack, A. M., van der Ploeg, L. H., Woods, S. C., and Seeley, R. J. (2000) Long-term orexigenic effects of AgRP-(83–132) involve mechanisms other than melanocortin receptor blockade. *Am. J. Physiol.: Regul., Integr. Comp. Physiol.* 279, R47–52.
- (11) Creemers, J. W., Pritchard, L. E., Gyte, A., Le, R. P., Meulemans, S., Wardlaw, S. L., Zhu, X., Steiner, D. F., Davies, N., Armstrong, D., Lawrence, C. B., Luckman, S. M., Schmitz, C. A., Davies, R. A., Brennand, J. C., and White, A. (2006) Agouti-related protein is posttranslationally cleaved by proprotein convertase 1 to generate agouti-related protein (AGRP)83–132: interaction between AGRP83–132 and melanocortin receptors cannot be influenced by syndecan-3. *Endocrinology* 147, 1621–1631.
- (12) Jackson, P. J., Douglas, N. R., Chai, B., Binkley, J., Sidow, A., Barsh, G. S., and Millhauser, G. L. (2006) Structural and molecular evolutionary analysis of Agouti and Agouti-related proteins. *Chem. Biol.* 13, 1297–1305.
- (13) McNulty, J. C., Thompson, D. A., Bolin, K. A., Wilken, J., Barsh, G. S., and Millhauser, G. L. (2001) High-resolution NMR structure of the chemically-synthesized melanocortin receptor binding domain AGRP(87–132) of the agouti-related protein. *Biochemistry* 40, 15520–15527.
- (14) McNulty, J. C., Jackson, P. J., Thompson, D. A., Chai, B., Gantz, I., Barsh, G. S., Dawson, P. E., and Millhauser, G. L. (2005) Structures of the agouti signaling protein. *J. Mol. Biol.* 346, 1059–1070.
- (15) He, L., Gunn, T. M., Bouley, D. M., Lu, X. Y., Watson, S. J., Schlossman, S. F., Duke-Cohan, J. S., and Barsh, G. S. (2001) A biochemical function for attractin in agouti-induced pigmentation and obesity. *Nat. Genet.* 27, 40–47.
- (16) Patel, M. P., Cribb Fabersunne, C. S., Yang, Y.-K., Kaelin, C. B., Barsh, G. S., and Millhauser, G. L. (2010) Loop-swapped chimeras of the agouti-related protein and the agouti signaling protein identify contacts required for melanocortin 1 receptor selectivity and antagonism. *J. Mol. Biol.* 404, 45–55.
- (17) Jackson, P. J., McNulty, J. C., Yang, Y.-K., Thompson, D. A., Chai, B., Gantz, I., Barsh, G. S., and Millhauser, G. L. (2002) Design, pharmacology, and NMR structure of a minimized cystine knot with agouti-related protein activity. *Biochemistry* 41, 7565–7572.
- (18) Tota, M. R., Smith, T. S., Mao, C., MacNeil, T., Mosley, R. T., van der Ploeg, L. H., and Fong, T. M. (1999) Molecular interaction of Agouti protein and Agouti-related protein with human melanocortin receptors. *Biochemistry* 38, 897–904.
- (19) Chai, B.-X., Neubig, R. R., Millhauser, G. L., Thompson, D. A., Jackson, P. J., Barsh, G. S., Dickinson, C. J., Li, J.-Y., Lai, Y.-M., and Gantz, I. (2003) Inverse agonist activity of agouti and agouti-related protein. *Peptides* 24, 603–609.
- (20) Jiang, L., Kimura, R. H., Miao, Z., Silverman, A. P., Ren, G., Liu, H., Li, P., Gambhir, S. S., Cochran, J. R., and Cheng, Z. (2010) Evaluation of a (64)Cu-labeled cystine-knot peptide based on agouti-related protein for PET of tumors expressing alphavbeta3 integrin. *J. Nucl. Med.* 51, 251–258.
- (21) Silverman, A. P., Kariolis, M. S., and Cochran, J. R. (2011) Cystine-knot peptides engineered with specificities for alpha(IIB)beta(3) or alpha(IIB)beta(3) and alpha(v)beta(3) integrins are potent inhibitors of platelet aggregation. *J. Mol. Recognit.* 24, 127–135.
- (22) Silverman, A. P., Levin, A. M., Lahti, J. L., and Cochran, J. R. (2009) Engineered cystine-knot peptides that bind alpha(v)beta(3) integrin with antibody-like affinities. *J. Mol. Biol.* 385, 1064–1075.
- (23) Duckert, P., Brunak, S., and Blom, N. (2004) Prediction of proprotein convertase cleavage sites. *Protein Eng. Des. Sel.* 17, 107–112.
- (24) Taylor, N. A., Van, D. V. W. J., and Creemers, J. W. (2003) Curbing activation: proprotein convertases in homeostasis and pathology. *FASEB J.* 17, 1215–1227.
- (25) Breen, T. L., Conwell, I. M., and Wardlaw, S. L. (2005) Effects of fasting, leptin, and insulin on AGRP and POMC peptide release in the hypothalamus. *Brain Res.* 1032, 141–148.
- (26) Flynn, M. C., Plata-Salaman, C. R., and French-Mullen, J. M. (1999) Neuropeptide Y-related compounds and feeding. *Physiol. Behav.* 65, 901–905.
- (27) Marks, D. L., Ling, N., and Cone, R. D. (2001) Role of the central melanocortin system in cachexia. *Cancer Res.* 61, 1432–1438.
- (28) Grossberg, A. J., Scarlett, J. M., and Marks, D. L. (2010) Hypothalamic mechanisms in cachexia. *Physiol. Behav.* 100, 478–489.
- (29) Reizes, O., Benoit, S. C., Strader, A. D., Clegg, D. J., Akunuru, S., and Seeley, R. J. (2003) Syndecan-3 modulates food intake by interacting with the melanocortin/AgRP pathway. *Ann. N.Y. Acad. Sci.* 994, 66–73.
- (30) Reizes, O., Lincecum, J., Wang, Z., Goldberger, O., Huang, L., Kaksonen, M., Ahima, R., Hinkes, M. T., Barsh, G. S., Rauvala, H., and Bernfield, M. (2001) Transgenic expression of syndecan-1 uncovers a physiological control of feeding behavior by syndecan-3. *Cell* 106, 105–116.
- (31) Zheng, Q., Zhu, J., Shanabrough, M., Borok, E., Benoit, S. C., Horvath, T. L., Clegg, D. J., and Reizes, O. (2010) Enhanced anorexigenic signaling in lean obesity resistant syndecan-3 null mice. *Neuroscience* 171, 1032–1040.
- (32) Wu, Q., Howell, M. P., Cowley, M. A., and Palmiter, R. D. (2008) Starvation after AgRP neuron ablation is independent of melanocortin signaling. *Proc. Natl. Acad. Sci. U.S.A.* 105, 2687–2692.
- (33) Yang, Y. K., Ollmann, M. M., Wilson, B. D., Dickinson, C., Yamada, T., Barsh, G. S., and Gantz, I. (1997) Effects of recombinant agouti-signaling protein on melanocortin action. *Mol. Endocrinol.* 11, 274–280.
- (34) Wilczynski, A., Wang, X. S., Joseph, C. G., Xiang, Z., Bauzo, R. M., Scott, J. W., Sorensen, N. B., Shaw, A. M., Millard, W. J., Richards, N. G., and Haskell-Luevano, C. (2004) Identification of putative agouti-related protein(87–132)-melanocortin-4 receptor interactions by homology molecular modeling and validation using chimeric peptide ligands. *J. Med. Chem.* 47, 2194–2207.